Metal dusting corrosion studies using thermogravimetric experiment coupled with acoustic emission analysis

Omar Al Haj, Véronique Peres, Eric Serris, Francois Ropital, François Grosjean, Jean Kittel, Michel Cournil

Publication in the journal 'Oxidation of Metals'(Peer-reviewed)

Metal dusting corrosion studies using thermogravimetric experiment coupled with acoustic emission analysis

Omar Al haj[a], Véronique Peres[a], Eric Serris[a], François Ropital[b], François Grosjean[b], Jean Kittel[b], Michel Cournil[a]

[a] *Ecole Nationale Supérieure des Mines, SPIN-EMSE, CNRS:FRE3312, LPMG, F-42023 Saint-Etienne, France.*
[b] *IFP Énergies nouvelles, Rond - point de l'échangeur de Solaize BP3 69360 Solaize France.*
alhaj@emse.fr; peres@emse.fr; serris@emse.fr; Francois.ROPITAL@ifpen.fr; Jean.KITTEL@ifpen.fr;

Francois.GROSJEAN@ifpen.fr; mcournil@emse.fr

Abstract The coupling of in situ physical techniques is a promising way to improve knowledge on the corrosion of metallic materials at high temperature. For this purpose thermogravimetric analysis (TGA) has been associated with acoustic emission (AE) devices to measure acoustic signals emitted during the corrosion of metal samples under carbon rich atmosphere ($a_c > 1$). Simultaneous measurements of the mass variation and of the acoustic signals can give complementary information to increase the level of understanding of metal dusting. This work presents the study of pure iron metal dusting corrosion at 600 °C under i-C_4H_{10} + H_2 + He atmosphere.

Keywords: Thermogravimetric analysis (TGA), Acoustic Emission (AE), Metal dusting, High temperature corrosion.

INTRODUCTION

Iron, nickel, cobalt and their alloys are broadly used in several industrial domains (aeronautics, nuclear …). Metal dusting is one of the catastrophic forms of high-temperature corrosion affecting these metals and their alloys when exposed to reducing gas atmospheres which are supersaturated with carbon. Be able to control the state of health of these metals and their alloys in service represents a major challenge for the industrials in various fields [1]. In order to quantify the degree of damage of these alloys, acoustic emission (AE) seems to be an interesting method owing to its sensivity and its non-destructive aspect. This non-destructive method detects the elastic energy liberated by materials. In the field of metal corrosion; this technique has mainly been employed to control generalized and localized corrosion of metallic materials immersed in electrolyte. Some studies have also used this technique to investigate materials behavior at high temperature. Ferrer et al. [2] studied by acoustic emission, the effect of dimethyl disulfide (DMDS) to inhibit metal dusting attack on sections of tube Incolloy 800. Acoustic emission experiments were performed by Schulte et al. [3] to evaluate the sulfidation of ferritic and austenitic steels. Bennett et al. [4] mounted an acoustic emission device in a thermobalance. Works were also carried out by Schmutzler et al. [5] on the study of oxidation mechanisms of Fe-Cr-Al by coupling TGA and AE. More recently, Tran et al. [6] also studied the oxidation of samples of titanium alloys in a tubular furnace instrumented with acoustic emission equipment. Acoustic emission can be applicable on equipments on line in service under various environmental conditions.

In this study we are interested in corrosion phenomena like coking, carburation and metal dusting existing in oil refining and in energy conversion industry (e.g. ethylene cracking), under carbon rich atmosphere.

Coking leads to the deposit of carbon at the surface of metal which can restrict thermal exchanges. Carburation is linked to the diffusion of carbon in metal which leads to the formation of metallic carbides. The metal dusting results in an important loss of metal thickness, sometimes widespread in form of holes (figure 1). It leads to the disintegration of metallic materials into a dust of fine metal particles and graphitic carbon. This corrosion phenomenon occurs in carburizing atmospheres, containing CO and/or hydrocarbons, at carbon activities greater than 1 ($a_c > 1$) [7, 8, 9, 10].

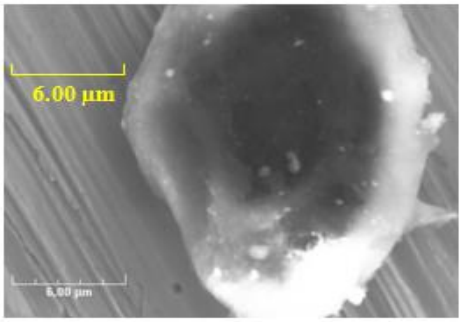

FIGURE 1: SEM picture : traces of coke in a hole due to metal dusting of the metal after carburization.

Metal dusting is generally explained by the following steps:

(1) Oversaturation of the metal phase with dissolved carbon, after the decomposition of hydrocarbons at the gas/metal interface.
(2) Nucleation and growth of cementite (Fe_3C) at the surface of metal but also at grain boundaries when the carbon activity is higher than the carbon activity for cementite formation ($a_c > a_{c\ (Fe/Fe3c)}$).
(3) As cementite limits carbon diffusion inside the metal, nucleation and growth of graphite takes place near the cementite while carbon activity a_c tends towards 1.
(4) In interaction with graphite, cementite becomes unstable and it decomposes to carbon and iron according to: $Fe_3C \longrightarrow 3\ Fe + C$. Carbon atoms attach to graphite planes, growing into the cementite. Iron atoms agglomerate to form fine particles, 20 nm average diameters.
(5) Iron particles act as catalyst for further carbon deposition and growth of carbon nanotubes, the coke is the combination of a catalytic particle and a graphite filament [11, 12, 13, 14, 15, 16].

Some of those steps, as cementite disintegration, are supposed to produce elastic energy in the material resulting in acoustic emissions.

This work presents metal dusting tests coupled with acoustic emission acquisition on pure iron samples.

EXPERIMENTAL PROCEDURES

Materials

The experiments were performed on iron samples provided by Weber (purity > 99.8 %). The chemical composition of these samples is presented in Table 1.

Table 1 Chemical analysis of the iron samples

Fe	C	Cr	Si	Al	Ti	Mo
Pure iron (+99,8%)	2 ppm	0.94 ppm	0.18 ppm	0.19 ppm	0.05 ppm	0.03 ppm

During the experimental tests, two specimen shapes were used, adapted to different locations on the acoustic waveguide:

1. Rectangular specimens (10 mm x 7 mm x 1 mm).
2. Samples in the form of a crescent moon with 15 mm diameter and 1 mm thick.

Specimens were cut by electrical discharge machining (EDM), and then they were mechanically polished to 1200 grit SiC, cleaned with ethanol and acetone.

Test Facility

Metal dusting experiments were carried out on a non-symmetric thermogravimetric analyzer (SETSYS TGA 92) equipped with a quartz furnace swept with a mixture of gazes (2.5 % i-C_4H_{10} + 2.5% H_2 + 95% He) which were

introduced by two flow meters. In order to quantify the impurities presented in the gas mixture, several measurements were done:
- The oxygen quantity was measured with an oxygen analyzer placed at the outlet of the thermobalance (Oxygen Analyzer series 900 EC 9, SYSTECH, accuracy ± 2% at 20°C) : 167 ppm.
- The water vapor pressure was measured by a high performance dew-point transmitter (OPTIDEW MICHELL with a high temperature sensor +130°C , accuracy ± 0.2°C dew point) : 0.7 mbar.
- The identification of gas species after their passage through the furnace was done using mass spectrometry analysis (Pfeiffer Vacuum, ThermoStar GSD 300 N2) to verify the thermal cracking at 600°C of isobutane (i-C_4H_{10}) and the catalytic effect of iron on this cracking. The decomposition of i-C_4H_{10} was confirmed following the formation of hydrocarbons impoverished in carbon (C_3H_8, C_2H_5, CH_4…) (figure 2).

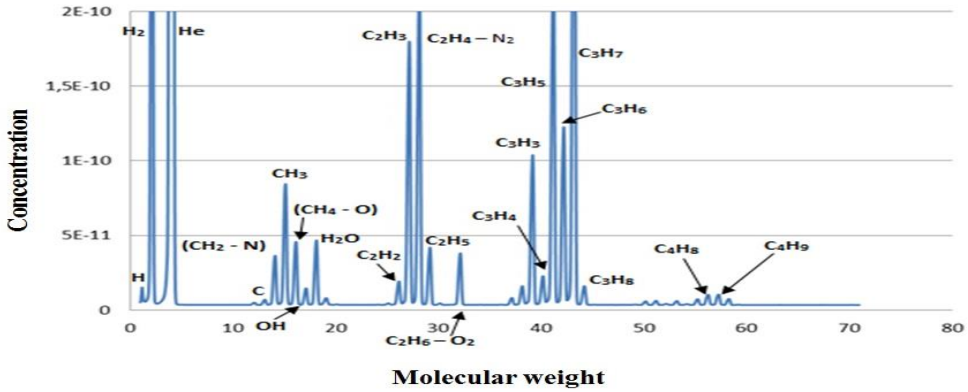

FIGURE 2: Mass spectrometry analysis of the gases at the outlet furnace during experiment at 600°C with an iron sample.

To register the acoustic signals emitted during the thermogravimetric experiment, a specific acoustic device has been developed (transducer, waveguide, acquisition chain). Its conception was limited by the internal diameter of the furnace and by the maximal weight that can be supported by the balance. The sample was put, but not directly linked, on the alumina waveguide with an optimized surface contact. AE transducers were placed inside the cold part of the thermobalance where temperature does not exceed 150 °C. The sensors are linked to an acquisition chain with characteristics given in Table 2. A normalized Hsu-Nielsen test (AFNOR NF EN 1330-9) was carried out to verify the AE system. This test simulates an acoustic emission event by breaking a 0.5 mm diameter pencil lead approximately 3 mm from its tip by pressing it against the surface of the sample. This generates an intense acoustic signal, quite similar to a natural AE source that the sensors detect as a strong burst. Generally, the lead breaks should generate amplitudes of at least 80 dB for a reference voltage of 1 mV and a total system gain of 80 dB. The signals resulting from our test present 90 dB amplitude. Blank tests without any specimen were carried out in order to check that the waveguide did not significantly react with the gas mixture; during these tests two kinds of signals were recorded: signals that appear during heating and signals which result from electronic noise (duration of 1µs and 1 count). These signals were been removed for the remainder of the study.

Table 2 Main characteristics of acoustic chain

Instrumentation	Data acquisition card	Filter of the preamplifier	Frequency (KHz)	Model of the amplifier
	PIC 2 2 chains	10 - 1200 KHz	300	2/4/6 gain : 40 dB

Test Conditions

Thermogravimetric analyses (TGA) were performed at 600 °C at atmospheric pressure (1 atm) with a gas flow rate of 4 $l.h^{-1}$ (2 $l.h^{-1}$ for 5% i-C_4H_{10} + 95% He and 2 $l.h^{-1}$ for 5% H_2 + 95% He). Those parameters correspond to a carbon activity of a_c = 81 137 (considering the reaction i-C_4 H_{10} ➔ 4 C + 5 H_2). To study the impact of water and

oxygen on the metal dusting mechanism, the first step of the experimental test (heating up to 600°C) was made under impure helium (H_2O, O_2) and under impure hydrogen (5% H_2 + 95% He +H_2O, O_2). Once the system reaches the isothermal (600°C) and isobaric (1 bar) state, we introduce the gas mixture (i-C_4H_{10} + H_2 + He) during a 12 hours plateau. Table 3 presents the main parameters of the two described tests.

Table 3 Test parameters

Experiment	Temperature rise under	Temperature	Plateau (time)	Sample Shape -Surface	AE AcquisitionThreshold
1	He	600°C	12 hours	Crescent moon - 28mm²	30 dB
2	H_2	600°C	12 hours	Rectangular plate 66 mm²	25 dB

RESULTS

Thermogravimetric Analysis (TGA)

The sample mass variations, normalized with the sample surface, as a function of temperature and time are presented respectively in figure 3 for heating up under helium and in figure 4 under hydrogen.
For the first test, there is an increase of mass gain at the beginning of the experiment followed by a decrease of mass gain following the introduction of reducing and carburizing gas mixture (i-C_4H_{10} + H_2 + He). Two hours after the introduction of the gas mixture, a second increase of mass gain is detected which has a quasi linear rate of 1.26 $g.m^{-2}.h^{-1}$. In the second test (figure 4), there is a less significant mass gain during the heating under hydrogen atmosphere followed by a small decrease of the mass sample when gas of test was introduced. Then during the soaking time, an increase of the mass gain is observed which has an average rate of 0.4 $g.m^{-2}.h^{-1}$.

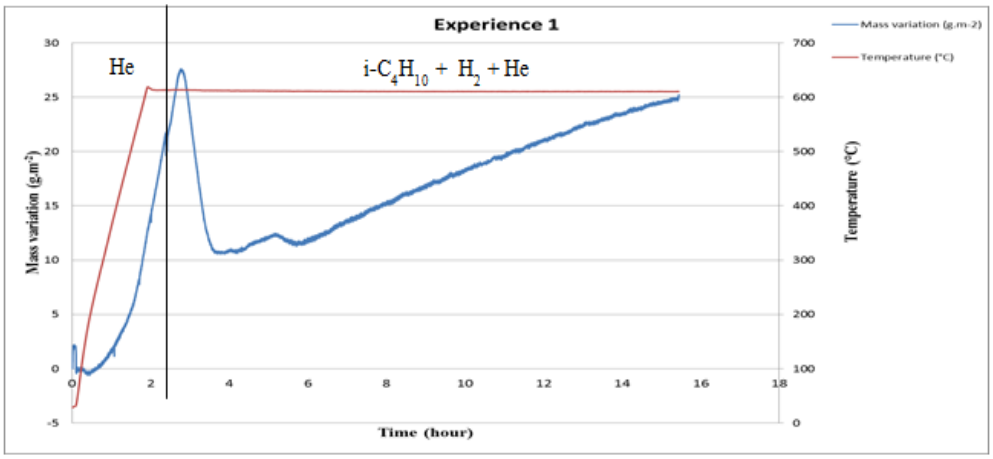

Figure 3: Sample mass variation for experiment 1, heating under He.

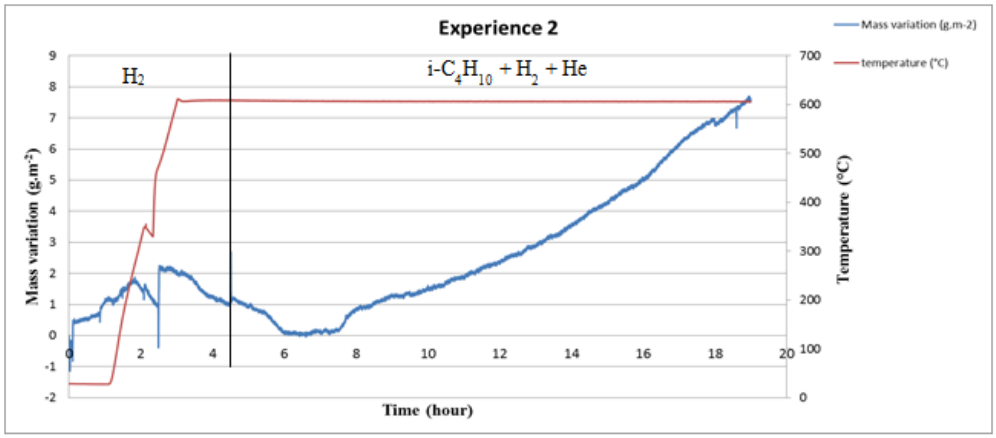

Figure 4: Sample mass variation for experiment 2, heating under H_2.

Sample Characterizations

For the two experiments, the corrosion behavior is not homogeneous on the two sample faces. The color of the face directly exposed to the carburizing gas flow is black. The reverse face color is gray. XRD analysis of the exposed sample surface after experiment 1 (Figure 5-a) indicates the presence of iron oxides (Fe_2O_3, Fe_3O_4) and some traces of iron carbide (Fe_2C). XRD diagram of the exposed sample surface for experiment 2 (Figure 5-b) reveals iron oxides (Fe_2O_3, Fe_3O_4) and cementite (Fe_3C) with some graphite traces.

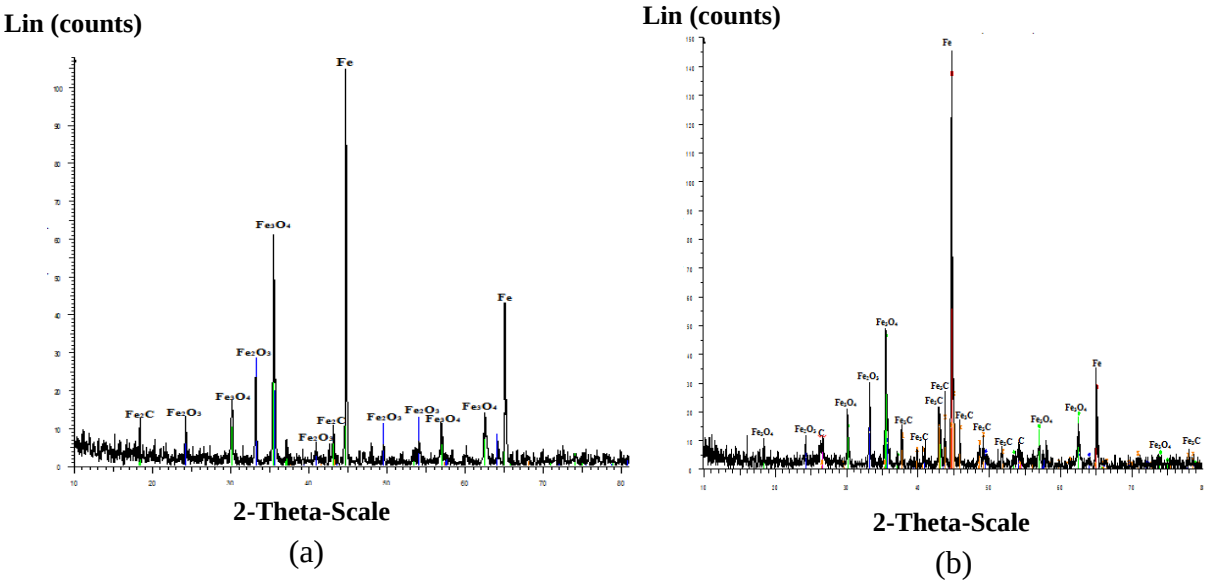

Figure 5: X-ray diffraction pattern from the external scale of the experience 1 (a) and the experience 2 (b).

Scanning electron microscopy (SEM-FEG) pictures of the carburized sample surfaces confirm the XRD analysis. Iron oxides phases are observed with some graphite deposits (figure 6 a-b) for the experience 1. Carbon nanotubes connected to iron catalyst particles have been observed which confirms the presence of coke during the experience 2 (figure 7 a-b-c).

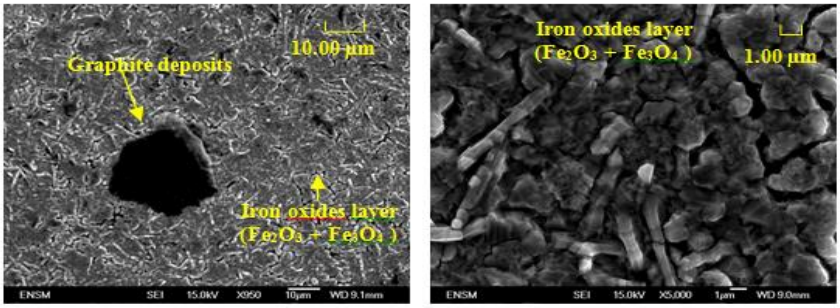

Figure 6: SEM pictures of the carburized iron surface in experiment 1.

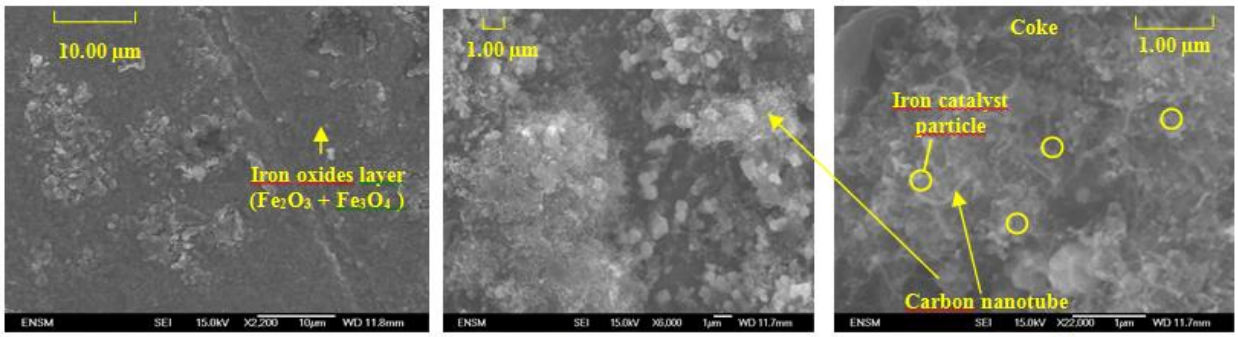

Figure 7: SEM pictures of the carburized iron surface in experiment 2.

Acoustic Emission Analysis (EA)

Acoustic emission signals have been recorded simultaneously during thermogravimetric analysis. The acoustic emission graphs (cumulated counts vs time) for the experiments 1 and 2 are presented figure 8. The respective acoustic emission acquisition thresholds are 30 dB and 25 dB.

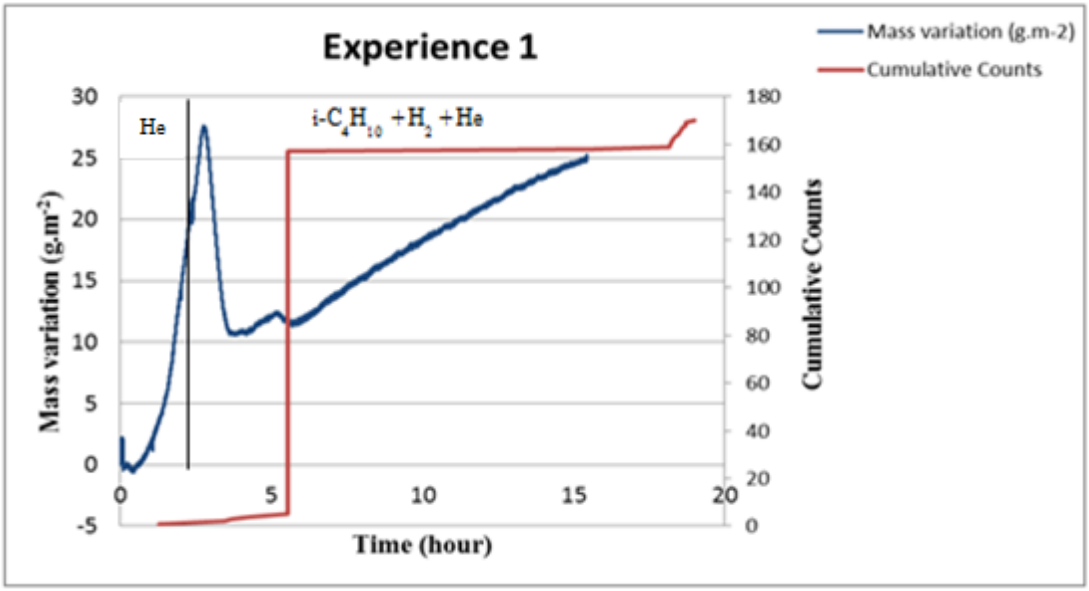

(a)

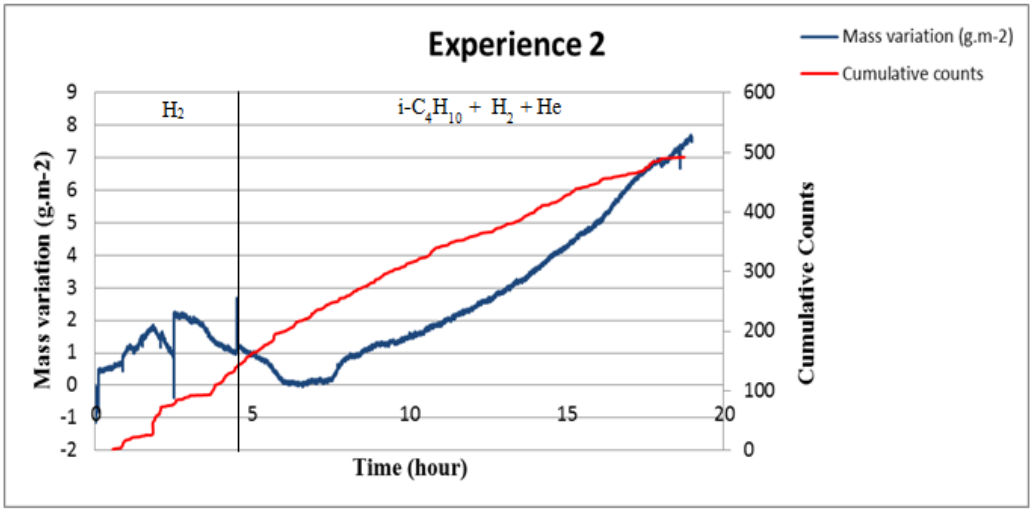

(b)

Figure 8: TGA and AE measurements for experiment 1 (a) and experiment 2 (b).

At the very beginning of experiment 1, some signals are observed corresponding to the heating of the furnace. Those signals are also visible in experiment 2 and in blank tests. The acquisition threshold has been lowered to 25 dB for experiment 2 in order to acquire more acoustic signals during the metal dusting process. Metal dusting appears to be an emitting corrosion mechanism in figure 8-b; a lot of signals are audible in between 25 and 30 dB during the soaking time at 600°C. Figure 9a and 9b show the EA signal amplitude versus duration of experiments 1 and 2. During experiment 2, with the reducing stage under hydrogen, the number of signals is more important and we observe some signals with longer duration up to 400µs.

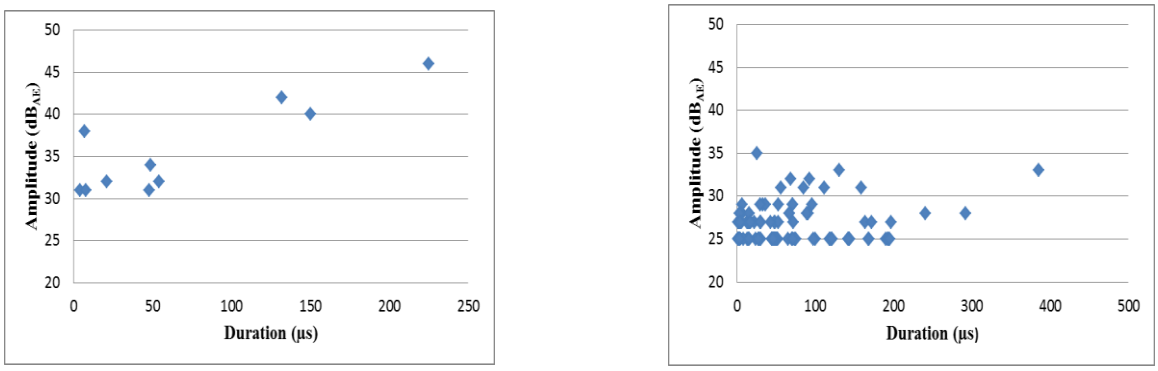

(a) (b)

Figure 9: Amplitude vs duration for experiment 1 (a) and experiment 2 (b).

Discussion

The iron sample mass gain observed during heating under helium with 167 ppm O_2 in experiment 1 corresponds to an oxidation of the iron sample surface which induces the growth of oxides phases (Fe_2O_3, Fe_3O_4). After this step, the carburized gas mixture (i-C_4H_{10} + H_2 + He) contributes to decrease the sample mass by the reduction of this iron oxides layer formed during the heating step. Following to the decomposition of i-$C_4H_{10,}$ after interaction with the

metal surface, carbon species diffuse into the iron matrix to form iron carbides (Fe_2C or Fe_3C). The AE measurements reveal that metal dusting is an emissive process.

During the heating phase under reducing gas mixture (5% H_2 + 95 % He - experiment 2), the thermogravimetric data show a limited oxidation of the iron sample, but the corrosion by oxygen cannot be completely avoided due to the low content of hydrogen imposed in the laboratory for safety reasons. After the introduction of the gas mixture ($i\text{-}C_4H_{10}$ + H_2 + He), the coking rate is about 0.4 $g.m^{-2}.h^{-1}$. This rate is three times lower than experiment 1's rate. This result may be interpreted by the oxidation process [17, 18] which occurs during the heating step (that leads to a more oxidized surface which is more reactive to coke deposition) but it can also depend on the sample orientation in the gas flow; the first sample has one face completely exposed to the process gaz, the second one was partially covered by the waveguide.

During experiment 2, the global metal dusting mechanism, cementite and coke formation, was confirmed by XRD and SEM analysis. The acoustic emission measurements reveal the presence of a significant number of acoustic signals during the coking phase. The attribution of the acoustic signals to the different emissive stages of metal dusting corrosion will need a detailed analysis of the wave forms and appropriate kinetics tests.

Conclusion

Pure iron samples have been exposed to carburized atmosphere in a thermogravimetric equipment coupled with an acoustic emission device. The experimental results confirm the major influence of the sample shape and positioning during the tests. A peculiar attention has to be done on the heating phase atmosphere, in order to take into account the oxygen potential which produces an oxidation step before the carburized one. In our test conditions, we cannot avoid the growth of the iron oxides layer. But the reducing step may be improved before the introduction of the carburized gas mixture. Metal dusting of iron samples seems to be an emissive corrosion phenomenon at high temperature. The results need to be confirmed and completed by a detailed study of the acoustic signals. The ultimate goal is to be able to attribute acoustic signals to the emissive stages of metal dusting.

REFERENCES

1. K. Ono, Acoustic emission, Encyclopedia of acoustics, Wiley, (1997).
2. F. Ferrer, J. Goudiakas, E. Andres and C. Brun, Nace Corrosion Conference, paper 01386 (2001).
3. M. Schulte, A. Rahmel and M. Schutze, *Oxidation of metals*, 49 pp.33 (1998).
4. M.J. Bennett, D.J. Buttle, P.D. Colledge, J.B. Price, C.B. Scruby and k.A. Stacey, *Materials Science and Engineering*, A120 199 (1989).
5. H. J. Schmutzler and H.J. Grabke, *Oxidation of metals*, **39** pp. 15- 29 (1992).
6. M.T. Tran, M. Boinet, A. Galerie , Y. Wouters, *Corrosion Science*, **52** pp. 2365–2371 (2010).
7. F. Ropital, Corrosion et dégradation des matériaux métalliques compréhension des phénomènes et application dans l'industrie pétrolière et des procédés, Editions Technip, Paris, pp. 73-79 (2009).
8. H.J. Grabke, High Temperature Corrosion and protection of Metals 5, Part 1, Mechanisms and prevention of Carbonaceous Gases, Volumes 369-372 pp. 101-107 (2000).
9. H.J. Grabke, M. Schütze, Corrosion by carbon and nitrogen: Metal dusting, carburisation and nitridation - European Federation of Corrosion (EFC) Series No. 41 pp. 1-23 (2007).
10. F. Ropital, P. Dascotte, P. Marchand, T. Faure, J.C. Lenain, A. Proust, Coupling Thermogravimetric and Acoustic Emission measurements: its application to study the inhibition of catalytic coke deposition, Eurocor, pp. 261 (2004).
11. G.W. Han, D. Feng, B. Deng, *Corrosion Science*, **46** , pp. 443-452 (2004).
12. D.J. Young, J. Zhang, C. Geers, M. Schütze**,** *Materials and Corrosion*, **62-1**, pp. 7-28 (2011).
13. J.C. Nava Paz and H.J.Grabke, *Oxydation of Metals*, **39**, pp. 437-456 (1993).
14. E.Pippel, J.Woltersdorf and H.J. Grabke, *Steel Research*, **66**, p.217 (1995).
15. C.M. Chun, T.A. Ramanarayanan and J.D. Mumford, *Mater. Corr.*, **50**, p. 634 (1999).
16. H.J. Grabke, E.M. Mûller-Lorenz, *Steel research* .**66**, pp. 252-258, (1995).
17. F. Grosjean, J. Kittel, F. Ropital, E. Serris, V. Peres, *Spectra analyse* **279**, pp. 35-44, (2011).
18. F. Bonnet, F. Ropital, Y. Berthier, P. Marcus, *Mater. Corr.*, **54**, pp. 870-880 (2003).